LJMU Research Online

Walmsley, A, Elton, S, Louys, J, Bishop, LC and Meloro, C

 Humeral epiphyseal shape in the felidae: The influence of phylogeny, allometry, and locomotion

http://researchonline.ljmu.ac.uk/id/eprint/493/

Article

For more information please contact researchonline@ljmu.ac.uk

Humeral Epiphyseal Shape in the Felidae: The Influence of Phylogeny, Allometry and Locomotion

Anthony Walmsley,[1] Sarah Elton,[2] Julien Louys,[3-4] Laura C. Bishop,[3] and Carlo Meloro[2]

[1]*Hull York Medical School, The University of York, Heslington York YO10 5DD, UK*

[2]*Hull York Medical School, The University of Hull, Loxley Building Cottingham Road, Hull HU6 7RX, UK*

[3] *Research Centre in Evolutionary Anthropology and Palaeoecology, School of Natural Sciences and Psychology, Liverpool John Moores University, Byrom Street, Liverpool L3 3AF, UK*

[4] *Present address: School of Earth Sciences, The University of Queensland, Brisbane, Australia*

Running Header:

FELID HUMERAL MORPHOLOGY

Correspondence: Carlo Meloro, Hull York Medical School, The University of Hull, Loxley Building, Cottingham Road, Hull HU6 7RX, UK; T: ++44 (0)1904 321918; F: ++44 (0)1482 466497; carlo.meloro@hyms.ac.uk

26 *ABSTRACT*

27 Bone morphology of the cats (Mammalia: Felidae) is influenced by many

28 factors, including locomotor mode, body size, hunting methods, prey size and

29 phylogeny. Here, we investigate the shape of the proximal and distal humeral

30 epiphyses in extant species of the felids, based on two-dimensional landmark

31 configurations. Geometric morphometric techniques were used to describe

32 shape differences in the context of phylogeny, allometry and locomotion. The

33 influence of these factors on epiphyseal shape was assessed using Principal

34 Component Analysis, Linear Discriminant functions and multivariate regression.

35 Phylogenetic Generalised Least Squares was used to examine the association

36 between size or locomotion and humeral epiphyseal shape, after taking a

37 phylogenetic error term into account. Results show marked differences in

38 epiphyseal shape between felid lineages, with a relatively large phylogenetic

39 influence. Additionally, the adaptive influences of size and locomotion are

40 demonstrated, and their influence is independent of phylogeny in most, but not

41 all, cases. Several features of epiphyseal shape are common to the largest

42 terrestrial felids, including a relative reduction in the surface area of the humeral

43 head and increased robusticity of structures that provide attachment for joint-

44 stabilising muscles, including the medial epicondyle and the greater and lesser

45 tubercles. This increased robusticity is a functional response to the increased

46 loading forces placed on the joints due to large body mass.

47

48 KEY WORDS**:** Felidae; humerus; geometric morphometrics; phylogeny;

49 allometry; locomotion

50

INTRODUCTION

52   Accounting for more than ten percent of extant mammalian Carnivora,

53 the Felidae are one of the most well-known families with well over 30 species

54 found on all continents apart from Antarctica and Australia where no endemic

55 species are recorded (Kitchener, 1991; Turner & Antón, 1997; Johnson et al.,

56 2006; MacDonald et al., 2010). All felids are hypercarnivorous, specialised

57 consumers of vertebrates (Kitchener, 1991; Turner & Antón, 1997; Kitchener et

58 al., 2010). This common behaviour has generated relatively conservative cranial

59 and mandibular morphology in the family when compared to other carnivorans

60 (Holliday & Steppan, 2004; Meloro et al., 2008, 2011; Werdelin & Wesley-Hunt,

61 2010; Meloro, 2011a, b; Meloro & O'Higgins, 2011). In the felid postcranial

62 skeleton, interspecific differentiation has been observed, in part because of

63 adaptations to locomotion and posture (Gonyea, 1976; Van Valkenburgh, 1987;

64 Anyonge, 1996; Andersson & Werdelin, 2003; Meachen-Samuels & Van

65 Valkenburgh, 2009a), but also to adaptations for procuring prey of different

66 sizes (Meachen-Samuels & Van Valkenburgh, 2009a, b, 2010; Lencastre

67 Sicuro, 2011; Lencaster Sicuro & Oliveira, 2011; Meachen-Samuels, 2012) and

68 due to specialisations for different modes of hunting (Christiansen, 2008; Slater

69 & Van Valkenburgh, 2008). Notwithstanding these studies, there is still much to

70 be explored regarding morphological variation in the felid postcranium and the

71 factors, including phylogeny and allometry, that contribute to it.

72   Felid-like mammals originated in the Oligocene, around 35 million years

73 ago. The earliest stem felid to be identified in the fossil record, *Proailurus*, was

74 recovered in the Quercy fissures (France) and is dated approximately 28.5 Ma.

75 Molecular data suggest that the modern family Felidae arose within the last 11

76 million years (Johnson et al., 2006; Werdelin et al., 2010). Based on molecular

77 evidence, the *Panthera* lineage (or clade), comprising the genera *Neofelis*

78 (clouded leopard) and *Panthera* (lion, jaguar, leopard, tiger, snow leopard) is

79 sister to all other extant members of the Felidae (Johnson et al., 2006). This

80 clade originated around six million years ago, with considerable speciation in

81 the genus *Panthera* occurring between around four and two million years ago

82 (Johnson et al., 2006). Three other lineages, the Leopard Cat, Bay Cat and

83 Caracal, diverged at the very end of the Miocene (5-6 Ma), with another, the

84 Puma, originating just less than five million years ago (Johnson et al., 2006).

85 The other lineages (Domestic Cat, Lynx, and Ocelot) diverged in the Pliocene,

86 around three million years ago (Johnson et al., 2006).

87   Even with a common adaptation to hypercarnivory, the felids

88 demonstrate a large range of body masses, a multitude of behaviours, and

89 marked ecological diversity (Ewer, 1973; Turner & Antón, 1997; MacDonald et

90 al., 2010). Members of the felid family range in size from under three kilograms

91 (e.g. the black footed cat, *Felis nigripes*) to over 300 kilograms (the tiger,

92 *Panthera tigris*). Felids exploit environments as diverse as open desert (e.g. the

93 sand cat, *Felis margarita*), rainforest (e.g. the jaguar, *Panthera onca*), grassland

94 (e.g. the lion, *Panthera leo*) and rocky, mountainous regions (e.g. the bobcat,

95 *Lynx rufus*). Since locomotor mode correlates with the habitat exploited, felids

96 show considerable diversity in locomotion, with some species engaging in

97 purely terrestrial locomotion and others demonstrating a high degree of

98 arboreality (Ewer, 1973; Kitchener, 1991; Kitchener et al., 2010).

99   Given the large size range within the felids, allometry is likely to play

100 some role in determining the shape of their postcranial skeletons (Mattern &

101 McLennan, 2000; Diniz-Filho & Nabout, 2009; Meachen-Samuels & Van

102 Valkenburgh, 2009a; Lewis & Lague, 2010). In addition, various studies have

103 implied that phylogeny influences bone morphology within both the carnivoran

104 cranium (Meloro et al., 2008, 2011; Meloro & O'Higgins, 2011) and postcranium

105 (Andersson & Werdelin, 2003; Meloro, 2011a). A small number of studies have

106 examined the relative importance of several factors determining postcranial

107 skeletal form in mammals (Monteiro & Abe, 1999; Young, 2008; Astúa,

108 2009),but most have focused on single contributory factors, such as locomotor

109 behaviour (Clevedon Brown & Yalden, 1973; Van Valkenburgh, 1987; Carrano,

110 1999; Schutz & Guralnick, 2007; Polly & MacLeod, 2008; Meloro, 2011c) or

111 allometry (Bertram & Biewener, 1990; Christiansen, 1999, 2002).

112   In this paper, we examine three factors - phylogeny, size and locomotion

113 – that, alongside other behaviours such as prey capture and foraging, are highly

114 likely to contribute to postcranial bone shape in the felids (Ewer, 1973; Van

115 Valkenburgh, 1987; Turner & Antón, 1997; Meachen-Samuels & Van

116 Valkenburgh, 2009a, 2010; Kitchener et al., 2010; Meachen-Samuels, 2012).

117 Our aim is to provide a detailed description of postcranial bone shape by

118 employing geometric morphometrics in order to quantitatively assess the impact

119 of these factors expressed as percentages of explained variance in shape (cf.

120 Caumul & Polly, 2005). Understanding the factors influencing shape is

121 important for successfully interpreting the evolutionary history and ecology of

122 this diverse family, and provides a quantitative framework for analysing fossil

123 species.

124   We focus on the humeral epiphyses partly because the humerus is

125 argued to reflect function, in both felids (Meachen-Samuels & Van Valkenburgh,

126 2009a, 2010; Lewis & Lague, 2010) and other mammals, including primates

127 and rodents (Elton, 2001, 2002, 2006; Samuels & Van Valkenburgh, 2008). As

128 in primates, the shoulder of many felids is highly mobile and can be used to

129 negotiate complex terrestrial and arboreal environments. Thus, the humerus is

130 often a much better indicator of subtle locomotor differences than hindlimb

131 bones, which tend to provide propulsion (Clevedon Brown & Yalden, 1973).

132 Since the forelimb is load bearing (Day & Jayne, 2007; Doube et al., 2009), the

133 humerus bone itself is also likely to be moulded by allometry, and one would

134 expect the largest felids to exhibit the most robust humeri (Doube et al., 2009;

135 Lewis & Lague, 2010). We thus have three specific research questions:

136   1. To what extent, if any, phylogeny explains shape variance in the felid

137 humeral epiphyses.

138   2. To what extent, if any, allometric scaling influences the shape of the

139 epiphyses.

140   3. To what extent, if any, function (specifically that related to locomotion)

141 influences the shape of the epiphyses.

142

143 **MATERIALS AND METHODS**

144 **Specimens and data collection**

145   Our sample comprised 110 humeri of 32 extant felid species, obtained

146 from collections held at the Natural History Museum London, the National

147 Museum of Scotland and the Royal Museum for Central Africa, with data

148 collected between June 2008 and July 2009 by Meloro. For each species we

149 included the following number of specimens (in parentheses): *Acinonyx jubatus*

150 (5), *Caracal caracal* (2), *Caracal aurata* (2), *Caracal serval* (6), *Felis chaus* (2),

151 *Felis silvestris lybica* (3), *Felis margarita* (2), *Felis nigripes* (2), *Felis silvestris*

152 *grampia* (9), *Lynx canadensis* (4), *Lynx lynx* (3), *Leopardus pardalis* (4), *Lynx*

153 *pardinus* (2), *Lynx rufus* (1), *Leopardus wiedii* (1), *Leopardus geoffroy* (2),

154 *Leopardus guigna* (1), *Neofelis nebulosa* (3), *Pardofelis badia* (1), *Pardofelis*

155 *marmorata* (1), *Pardofelis temminckii* (1), *Prionailurus bengalensis* (4), *Puma*

156 *concolor* (2), *Puma jagouaroundi* (1), *Panthera leo* (17), *Panthera onca* (3),

157 *Panthera pardus* (12), *Panthera tigris* (4), *Panthera uncia* (4), *Prionailurus*

158 *planiceps* (1), *Prionailurus rubiginosus* (1), *Prionailurus viverrinus* (4). Details

159 about the studied material are listed for each individual skeletal element in

160 Supplementary online material Table 1.

161   Two-dimensional images of the humeral epiphyses were captured using

162 a Nikon d40 digital camera with a 200mm lens following a standard protocol.

163 Specimens were placed at a minimum focal distance of one metre from the

164 camera attached to a Manfrotto tripod. A spirit level was used to ensure that the

165 top of the camera remained perpendicular to the specimen being photographed.

166 Eighty two of the 110 images were of the left humerus; the remaining images, of

167 right humeri, were flipped horizontally in tpsDig (version 2.12, Rohlf, 2008) prior

168 to landmarking and analysis. The proximal epiphysis was photographed from

169   medial and lateral aspects, and the distal epiphysis from anterior and posterior

170   aspects. Data for the distal epiphysis were obtained for all 110 specimens,

171   whereas proximal data were obtained for only 109 specimens.

172   Landmarks describing the shape of each epiphysis were digitised by

173   Walmsley in tpsDig (Rohlf, 2008) (Fig. 1). Given the potential for increasing

174   statistical error when using Procrustes methods with relatively small sample

175   sizes (Rohlf, 2000, 2003a; Cardini & Elton, 2007), accuracy and precision of

176   landmarking and consequently the amount of digitisation error were assessed.

177   To do this, four specimens, chosen to represent the range of body masses of

178   species in the study, were selected for further landmarking. Two of these,

179   *Leopardus geoffroyi* and *Pardofelis temminckii*, represented species lying within

180   modal frequencies, another belonged to the species with the largest body mass,

181   *Panthera leo*, and the fourth to the species with the smallest body mass,

182   *Prionailurus rubiginosus*. Over a period of three days, each specimen was

183   landmarked according to the scheme illustrated in Fig. 1. Landmarking was

184   repeated a further three times during this period, producing a total of four

185   configurations per specimen. By calculating linear distances between landmarks

186   and assessing how these distances changed after each successive

187   landmarking, it was determined that error due to digitisation was minimal and

188   that landmarks could be repeated with confidence (Supplementary online

189   material Table 2).

190

191   **Data analysis – Geometric morphometrics (GMM)**

192   The software *morphologika* (O'Higgins & Jones, 2006) was used to

193 conduct Generalised Procrustes Analyses (GPA) and Principal Component

194 Analyses (PCA). GPA superimposes the raw coordinates of each landmark

195 configuration by removing the effects of translation and rotation, and also scales

196 these configurations by calculating a unit centroid size (defined as 'the square

197 root of the sum of squared Euclidean distances from each landmark to the

198 centroid of the landmarks') for each specimen (Bookstein, 1989; Adams et al.,

199 2004; Zelditch et al., 2004). After GPA the landmark configurations provided by

200 each specimen lie within the non-Euclidean, Kendall shape space. Specimens

201 are distributed about the mean landmark configuration and are spread

202 throughout this space according to differences in shape (Zelditch et al., 2004;

203 Chen et al., 2005). To analyse shape differences further, the spread of data

204 within the non-Euclidean space is projected onto a Euclidean, linear tangent

205 space (Rohlf, 1996). Interpretation of the resulting shape data requires PCA.

206 This method of analysis provides orthogonal axes (Principal Components, PCs)

207 that successively describe the major aspects of variance of the sample. With

208 the use of mean coordinates plus eigenvectors, PCA allows shape variance for

209 each PC to be demonstrated graphically (Zelditch et al., 2004; Chen et al.,

210 2005). In the present sample, analyses conducted using tpsSmall version 1.20

211 (Rohlf, 2003b) indicated there was a very strong correlation ($r = 0.999$) between

212 non-Euclidean and Euclidean tangent space. Thus, the linear tangent space

213 demonstrated by the PC plots reliably describes shape variance amongst

214 specimens.

215

Phylogeny

Specimens were grouped according to lineage (Johnson et al., 2006, Supplementary online material Table 1) in order to assess the extent of phylogenetic influence on shape. For each epiphyseal aspect, plots of PC1 vs. PC2 were produced. The shape variance demonstrated by the PC plots was visualised via transformation grids. These transformation grids, formed using thin plate splines, show the relative deformation of structures (Bookstein, 1991), in this case across each PC. The relationship between phylogenetic lineage and shape was investigated by creating dummy variables for each lineage, which were regressed against the multivariate shape data (all PCs). This determined the correlation between phylogeny and shape using a test equivalent to a MANOVA (multivariate analysis of variance), with significance calculated via the Wilks' Lambda test. This test, performed for each aspect of the whole sample (N=109 or 110) in tpsRegr version 1.37 (Rohlf, 2009), also indicates the percentage of shape variance explained by phylogeny.

Allometry

The influence of allometry on shape variance was investigated via multivariate regression (Monteiro, 1999) performed in *morphologika* (O'Higgins & Jones, 2006). Natural log (NLog) transformed centroid size values were regressed against all PCs collectively, with significance computed using the Wilks' Lambda. Transformation grids were used to illustrate changes in shape from the median sized specimens to the smallest and largest (based on NLog centroid size values).

240

Locomotion

242   Similar methods to those employed in the phylogeny multivariate

243 regression were used to examine the relationship between locomotor mode and

244 shape. Species were assigned to one of three locomotor categories,

245 'Terrestrial', 'Terrestrial but Climbs' and 'Terrestrial and Arboreal'

246 (Supplementary online material Table 1), based on classifications in Ortolani &

247 Caro (1996). Dummy variables for the three locomotor groups were regressed

248 against shape. Additionally, discriminant function analysis (DFA) was used to

249 explore the changes in shape, as well as size, across locomotor categories.

250 Both shape (PCs) and size (NLog centroid size) variables were used in

251 discriminant analyses, performed for each epiphyseal aspect in PASW version

252 18 (SPSS Inc., 2009) using a stepwise method (variables are entered into the

253 model if the significance level of their F value is less than 0.05, and they are

254 removed if the significance level is greater than 0.01) to select the variables

255 which best discriminate locomotor categories. Following a recent study (Meloro,

256 2011a), size has been included alongside shape variables (cf. Schultz &

257 Guralnick, 2007) to increase prediction likelihood of ecological categories. The

258 locomotor categories assigned *a priori* were the same as those used in the

259 regression analyses. Shape variance across each function was visualised by

260 regressing discriminant function scores against shape variables in tpsRegr

261 version 1.37 (Rohlf, 2009), with transformation grids at either extreme of the

262 axes demonstrating deformation from the mean shape. The locomotor groups of

263 the unclassified/unknown specimens were predicted based on data provided by

264   the discriminant functions. A 'leave-one-out' procedure was conducted as a

265   cross validation.

266

267   **Sensitivity analyses**

268   In order to validate the efficacy of our discriminant models, to make

269   predictions irrespective of unequal taxonomic sample size (Kovarovic et al.,

270   2011), we performed two kinds of sensitivity analyses. First, we repeated the

271   most accurate DFA after removing from the original sample all the specimens

272   belonging to a particularly abundant taxon. We repeated the DFA by excluding

273   first *Panthera leo* (N = 17, the most abundant 'Terrestrial' felid), then *Felis*

274   *silvestris grampia* (N = 9, the most abundant 'Terrestrial but Climbs'), and finally

275   *Neofelis nebulosa* (N = 3, representative of 'Terrestrial and Arboreal').

276   A second sensitivity analysis was conducted to test for the effect of

277   sample size (number of specimens) or body mass (in grams, log transformed)

278   on percentage of correctly classified specimens for the 32 extant species

279   sampled. Non-parametric Spearman correlation was applied to identify positive

280   or negative significant correlations based on the results from all the DFA

281   models.

282

283   **Phylogenetic Generalised Least Squares (PGLS)**

284   PGLS regressions were performed for each epiphyseal aspect, to assess

285   if differences in shape between specimens as described by locomotion or

286   allometry alone were independent of phylogeny (or specifically whether they

287   were independent of the lineage to which they belong). This method, which can

288   also be used for multivariate datasets, incorporates phylogeny as an error term

289   within the regression models of shape variables on locomotion (transformed into

290   dummy variables) or size (Martins & Hansen, 1997; Rohlf, 2001, 2006a; Adams,

291   2008). For these analyses, we computed the mean shape coordinates for each

292   species, performing separate GPAs for each species subsample (cf. Meloro et

293   al., 2008). Size for each species was represented by NLog centroid size

294   averaged from multiple specimens. The phylogenetic covariance matrix was

295   computed based on the topology and time of divergence (from Johnson et al.,

296   2006) and then added as error term in the multivariate regression models in

297   NTSYS 2.21c (Rohlf, 2006b).

298

299   **RESULTS**

300   **Phylogeny**

301   MANOVA indicates that shape differs significantly between lineages

302   (Table 1). Phylogeny accounts for the greatest shape variance for the anterior

303   aspect of the distal epiphysis and least for the medial aspect of the proximal

304   epiphysis. For the lateral aspect of the proximal epiphysis, PC1 and PC2

305   collectively describe 88.09% of the shape variance (PC1, 58.93%; PC2,

306   29.16%) (Fig. 2A). Even though some overlap between lineages is evident, the

307   Puma lineage tends to cluster at more negative PC1 values, whereas Ocelot,

308   Leopard Cat and Domestic Cat lineages have more positive values. Specimens

309   having extreme negative scores on PC1 have a greater tubercle that projects

310   superiorly above the humeral head, and a humeral head with little posterior

311   projection, whilst specimens with positive scores have a more superiorly and

312   posteriorly projecting humeral head with a wider articular surface. Lineages

313   overlap more on PC2, which describes the antero-posterior expansion of the

314   greater tubercle associated with reduction of the articulating area of the

315   humerus head (Fig. 2A).

316   For the medial aspect of the proximal epiphysis, PC1 and PC2 explain

317   69.07% of the shape variance (PC1, 35.99%; PC2, 33.08%). Overlap occurs

318   between lineages on both axes (Fig. 2B). However, specimens belonging to the

319   *Panthera* and Domestic Cat lineages exhibit negative PC1 and PC2 scores

320   respectively (Fig. 2B). PC1 describes variation in the posterior projection of the

321   humeral head associated with variation in the width of the lesser tubercle. On

322   PC2, specimens with the most negative scores have a more posteriorly

323   projecting humeral head and a greater tubercle with relatively little projection in

324   the superior plane.

325   For the anterior aspect of the distal epiphysis, PC1 and PC2 collectively

326   describe 72.94% of the shape variance (PC1, 62.69%; PC2, 10.25%). All

327   lineages tend to cluster well along PC1, although Ocelot specimens cluster

328   better on PC2 (Fig. 2C). On PC1, specimens at the positive end of the axis

329   have a more proximally positioned supracondyloid foramen and a relatively

330   smaller combined medio-lateral width of the trochlea and capitulum. On PC2,

331   from negative to positive, there is a relative superior-inferior expansion of the

332   trochlea and capitulum (Fig. 2C).

333   For the posterior aspect of the distal epiphysis, PC1 and PC2 collectively

334   describe 56.72% of the shape variance (PC1, 36.40%; PC2, 20.32%). Some

335   lineage-based clustering is evident (Fig. 2D), with *Panthera* specimens, for

336 example, being at the more positive end of PC1, with a relatively larger

337 olecranon fossa area and relatively smaller trochlea/capitulum in the superior-

338 inferior dimension. From negative to positive PC2 scores there is a relative

339 reduction in the medial projection of the medial epicondyle and a decrease in

340 the width of the distal portion of the trochlea and capitulum plus an expansion in

341 olecranon fossa area.

342

343 **Allometry**

344   In multivariate regression, NLog centroid size was significantly correlated

345 with shape for both aspects of each epiphysis (Table 2). Allometry explains

346 more shape variance in the anterior aspect of the distal epiphysis than in the

347 posterior aspect, and more in the lateral aspect of the proximal epiphysis

348 compared to the medial. Shape changes in relation to changes in NLog centroid

349 size values are illustrated in Fig. 3. On the lateral aspect of the proximal

350 epiphysis, as NLog centroid size increases, there is a decrease in the humeral

351 head surface area and a slight increase in the proximal projection of the greater

352 tubercle (Fig. 3A). Inspection of transformation grids for the medial aspect of the

353 proximal epiphysis (Fig. 3B) indicates that larger specimens have a relatively

354 larger lesser tubercle. On the anterior aspect of the distal humerus (Fig. 3C),

355 larger specimens have a relatively larger combined width of trochlea and

356 capitulum with a shorter and broader medial epicondyle. Differences on the

357 posterior aspect of the distal epiphysis are less marked, although specimens

358 with high NLog centroid size values show an increase in the olecranon fossa

359 area (Fig. 3D).

360

Locomotion

MANOVA indicates that shape differs significantly between locomotor categories for both proximal and distal epiphyses although, in general, locomotor differences account for much less shape variance than do either phylogeny or allometry (Table 3). In DFA, two significant functions were extracted for each aspect except the posterior distal epiphysis (Table 4). Table 5 lists the variables selected after the stepwise for the DFA models, with NLog centroid size being included in three of the four models. Reclassification rates using the 'leave one out' method (Table 6) were above chance for each aspect of the epiphyses, with the anterior aspect of the distal epiphysis being the region that best discriminated between different locomotor groups.

The DFA plots show some discrimination between locomotor groups even if overlap occurs among specimens (Fig. 4). Terrestrial specimens tend to occupy positive scores of DF1 in all structures except in the anterior aspect of the distal epiphysis (Fig. 4C). For the proximal epiphysis positive scores of DF1 are associated to short articular surface and a wide lesser tubercle (Figs. 4A, B). 'Terrestrial and Arboreal' specimens tend to occupy positive scores of Function 2 for the lateral aspect of the proximal epiphysis, characterised by less superiorly projecting humeral head (Fig. 4A). However, they overlap extensively with 'Terrestrial but Climbs' specimens and this is reflected in the re-classification rate (Table 6).

For the distal epiphysis, terrestrial specimens have positive scores of DF1 that describe a relatively wide medial epicondyle and a large medio-lateral

384   width of the trochlea (Fig. 4C). Interestingly, Terrestrial and Arboreal specimens

385   share a wider medial epicondyle with a larger superior-inferior dimension of the

386   trochlea and the supracondyloid foramen on the anterior aspect of the distal

387   epiphysis (Fig. 4C). The posterior aspect of the distal epiphysis does not

388   differentiate locomotor groups on either function (Fig. 4D).

389   As the medial aspect of the proximal epiphysis and the anterior aspect of

390   the distal epiphysis are the best predictors of locomotor category (Table 6), the

391   functions formed by their shape and size variables are used to predict the

392   locomotor categories for the four specimens of unclassified/unknown

393   locomotion. In the case of the medial aspect of the proximal epiphysis,

394   *Pardofelis badia* and *Pardofelis temminckii* are classified as 'Terrestrial and

395   Arboreal' and both *Felis nigripes* specimens are classified as 'Terrestrial but

396   Climbs'. For the anterior aspect of the distal epiphysis, *Pardofelis badia* and

397   both *Felis nigripes* specimens are classified as 'Terrestrial and Arboreal',

398   whereas *Pardofelis temminckii* is classified as 'Terrestrial but Climbs'.

399

400   **Sensitivity Analyses**

401   The percentage of correctly classified specimens differs between species

402   (Table 7). With regard to species with more than one representative specimen,

403   the lion (*Panthera leo*), the snow leopard (*Panthera uncia*) and the cheetah

404   (*Acinonyx jubatus*) appear to be the best classified in the analyses. There is a

405   significant association between body size and number of specimens per

406   species ($r = 0.62$, $p=0.0003$), but no other factor, including lineage and sample

407   size, affects the reclassification rate.

408   Separately excluding *Panthera leo*, *Neofelis nebulosa* and *Felis silvestris*

409   specimens (representing the species of largest sample size for each locomotor

410   group) from the discriminant function analyses, does not have a major impact

411   on the reclassification rate of the original DFA models (Table 8). In all cases,

412   the repeated DFA models are statistically significant. There is a small degree of

413   change however, with the exclusion of *Panthera leo* decreasing the

414   reclassification rate for both aspects of proximal epiphyses, whilst removing the

415   *Felis silvestris* sample improved models based on the lateral aspect of proximal

416   epiphysis and the posterior aspect of distal epiphysis. The exclusion of the only

417   three specimens of *Neofelis nebulosa* generally improved reclassification in all

418   the models except for anterior aspect of the distal epiphysis (Table 8).

419

420   **PGLS**

421   The PGLS models (Table 9), which incorporate phylogeny as an error

422   term, indicate that allometry has a significant independent influence on humeral

423   epiphyseal shape, except for the anterior aspect of the distal epiphysis.

424   Locomotion has a significant independent influence on the shape of the humeral

425   epiphyses, with the exception of the medial aspect of the proximal epiphysis.

426

427   **DISCUSSION**

428   In common with previous research on the felid postcranium (Van

429   Valkenburgh, 1987; Andersson & Werdelin, 2003; Andersson, 2004;

430   Christiansen & Harris, 2005; Doube el al., 2009; Meachen-Samuels & Van

431   Valkenburgh, 2009a), we find clear interspecific variation in long bone

432   morphology. Phylogeny, allometry and locomotion all influence humeral

433   epiphyseal shape in our sample, with phylogeny and allometry contributing

434   more than locomotion.

435   Phylogenetic signals in postcranial and cranial shape have been noted

436   among Carnivora as a whole (Radinsky, 1981; Andersson & Werdelin, 2003;

437   Andersson, 2004; Meloro et al., 2008, 2011; Meloro, 2011a, b, c; Meloro &

438   O'Higgins, 2011; Slater & Van Valkenburgh, 2008). MANOVA and PCA in the

439   present study indicate a marked phylogenetic signal in the shape of the humeral

440   epiphyses within the Felidae. For the shape of each aspect of both epiphyses

441   the *Panthera* lineage emerges as one of the most distinctive. This maybe a

442   result of its early divergence from all other cat lineages (Johnson et al., 2006).

443   Such distinctiveness has also been noted in ecomorphological analyses of felid

444   skulls (Werdelin, 1983; Slater & Van Valkenburgh, 2008; Lencastre Sicuro,

445   2011; Lencastre Sicuro & Oliveira, 2011) and it is apparent when mapping

446   averaged PC1 scores for all the four epiphyseal aspects onto the phylogenetic

447   topology (Fig. 5).

448   In PCA, members of the *Panthera* lineage tend to form a coherent group

449   separated from most other specimens. This is particularly striking given that the

450   group comprises purely terrestrial, terrestrial with climbing and mixed terrestrial

451   and arboreal species, with a large body mass range (some species being over

452   150 kg and others under 20kg). However, this diversity is evident in the PC

453   plots and mapping (Figs. 2 and 5). Although the lineage clusters have relatively

454   little overlap with other lineages, wide ranges of scores are still obtained for

455   *Panthera* specimens, for both aspects of the proximal humerus and the

456 posterior aspect of the distal humerus. This reflects the biological and ecological

457 diversity of modern members of the lineage, which speciated rapidly in the

458 Pliocene (Johnson et al., 2006). Among the other felid lineages, there is

459 considerable overlap on the plots of PC1 versus PC2. Members of the non-

460 *Panthera* lineages tend to be relatively small (17 out of the 26 non-*Panthera*

461 lineage species sampled are under 10kg), and that may account for some

462 overlap, especially since lineages mostly comprising small species tend to be

463 dominated by climbing or arboreal forms, which may create additional

464 convergence. Based on PC1 character mapping, this occurs consistently in the

465 'Leopard Cat' and 'Domestic Cat' lineages that show a limited variation

466 especially in the lateral aspect of proximal epiphysis and anterior aspect of the

467 distal epiphysis (Fig. 5).

468   The influence of size on cranial and postcranial morphology has been

469 noted within and between several families of the order Carnivora (Schutz &

470 Guralnick, 2007; Meloro et al., 2008, 2011; Meachen-Samuels & Van

471 Valkenburgh, 2009b; Meloro 2011b). In this study, allometry was a significant

472 influence on humeral epiphyseal shape (accounting for 17–40% of variance),

473 independent of phylogeny for all but the anterior aspect of the distal epiphysis.

474 Allometry explained a reasonably large amount of shape variance for the lateral

475 aspect of the proximal epiphysis. The largest specimens require the greatest

476 amount of stability at the joint to account for increased loading forces. These

477 demonstrate a reduced humeral head surface area, limiting the degree of

478 movement at the shoulder joint, and a more superiorly projecting greater

479 tubercle to reduce rotational movement and to provide a greater surface area

480   for insertion of the stabilising rotator cuff muscles (Kappelman, 1988; Turner &

481   Antón, 1997).

482   The shape of the anterior aspect of the distal epiphysis in larger specimens may

483   demonstrate adaptations for stability, including an increased projection of the

484   medial epicondyle for the attachment of muscles that allow pronation-supination

485   as well as flexing digits (i.e. M. pronator teres; M. palmaris longus; third and

486   fourth parts of M. flexor profundus digitorum; M. flexor carpi radialis; second

487   head of M. flexor profundus digitorum; page 171, Reighard & Jennings, 1901).

488   The elbow joint is load bearing, and it has been demonstrated that felid limbs

489   respond to increased body size, and therefore increased loading, via allometric

490   shape change (Doube et al., 2009), so larger species and specimens are more

491   robust. In felids the influence of allometry has been suggested to be much

492   stronger at the epiphyses than at the shaft, due to tension from muscle and

493   ligament attachments and due to shear and torsion from joint loading (Doube et

494   al., 2009). This allometric pattern is unique to felids, as other carnivoran families

495   (with species exhibiting body masses of less than 300 Kg), such as canids,

496   respond to an increase in body size by limb straightening (Day & Jayne, 2007;

497   Meachen-Samuels & Van Valkenburgh, 2009a).

498   Interestingly, PGLS shows that size influence is dependent on phylogeny

499   in the anterior aspect of distal epiphysis, suggesting that there is a very strong

500   phylogenetic signal in this region of the bone. The significant independent

501   contribution of locomotion in influencing the anterior distal humerus morphology

502   suggests that there has also been strong selective pressure on this region that

503   is not simply explained by size or conserved morphology. The assertion of

504 strong selective pressure for the anterior distal epiphysis is reinforced by the

505 reasonably high classification accuracy in discriminant analysis across all

506 locomotor groups (in general, better than the proximal epiphysis or posterior

507 distal aspect for all locomotor categories).

508   DFA and PGLS indicate that locomotion influences humeral epiphyseal

509 shape, further confirming the association between locomotion and mammalian

510 postcranial shape noted in previous studies (Van Valkenburgh, 1987;

511 Kappelman, 1988; Gebo & Rose, 1993; Plummer & Bishop, 1994; Elton, 2001,

512 2002; Schutz & Guralnick, 2007; Meachen-Samuels & Van Valkenburgh,

513 2009b; Meloro 2011a). This notwithstanding, locomotion explained the least

514 amount of humeral epiphyseal shape variance (between 5 and 16%) in our

515 sample. For the medial aspect of the proximal epiphysis, for which locomotion

516 explained the least variance (5%), PGLS indicated that this influence was

517 dependent on phylogeny.

518   The mean reclassification rate for the whole DFA was 65%, relatively

519 modest compared to studies of other mammals (Kappelman, 1988; Plummer &

520 Bishop, 1994; Bishop, 1999; Elton, 2001), but similar to the rate observed in an

521 earlier study (Meachen-Samuels & Van Valkenburgh, 2009a) of felid forelimb

522 shape that used a different locomotor categorisation system that divided the

523 sample into terrestrial, arboreal and scansorial specimens. Based on data from

524 Ortolani & Caro (1996), the majority of cats are at least partially terrestrial,

525 which may have assisted their extensive dispersal and cosmopolitan range

526 (sensu Hughes et al., 2008). This widespread terrestriality across species

527   inevitably results in morphological similarity, either because of shared ancestry

528   or convergence, which in turn is reflected in the discriminant analysis.

529   The DFA classification accuracy rate for the anterior aspect of the distal

530   epiphysis was surprisingly high in the 'Terrestrial but Climbs' category, given the

531   range of species and body masses included and in marked contrast to the

532   modest classification rates of the other humeral aspects for this category. The

533   landmark set for the anterior aspect of the distal humerus captures two

534   important components of the elbow joint: the trochlea, which articulates with the

535   ulna and the capitulum which articulates with the radial head, as well as the

536   medial epicondyle, the origin for mm. flexor carpi radialis, mm. flexor carpi

537   ulnaris, mm. flexor digitorum superficialis (all flexors of the manus) and the

538   manual pronator mm. pronator teres (Kardong & Zalisko, 2002). It is possible

539   that the good separation between 'Terrestrial but Climbs' and other felid

540   specimens reflects differences in manual flexion and pronation in climbing cats.

541   Discrimination was poor for the posterior aspect of the distal epiphysis, a result

542   consistent with the multivariate regression. Given the results for the anterior

543   aspect of the distal humerus, this result may seem anomalous, as the anterior

544   and posterior aspects are part of the same structure. However, the dominant

545   feature of the posterior distal humerus, the olecranon fossa, has been shown in

546   previous studies, albeit in primates, to be highly morphologically variable (Elton,

547   2001).

548   For the proximal humerus, as well as the posterior distal epiphysis, large

549   scatters around centroids were evident, with extensive overlap between

550   categories. In our study, there was reasonably high general classification

551 accuracy in the 'Terrestrial' sample. This reflects, in part, adaptations for

552 terrestriality (including a humeral head with a relatively decreased surface area,

553 and an increased lesser tubercle width and greater tubercle projection for

554 insertion of the rotator cuff muscles) which stabilise the limb and constrain

555 movement mainly to the parasagittal plane, important when chasing prey in

556 open environments (Kappelman, 1988; Gebo & Rose, 1993; Turner & Antón,

557 1997).

558 Additionally, our sensitivity analyses demonstrate that DFA models were

559 always accurate irrespective of sample size and species selection.

560 Classification rate varies across species but this variation has no pattern and is

561 not systematically influenced by any ecological or phylogenetic factor. On the

562 other hand, the exclusion of particular taxa from our sample confirms DFA

563 model stability, where accuracy appears to be unchanged or even increased in

564 some cases. This allows us to interpret with confidence the classification of

565 unknown specimens. The classification of *Pardofelis badia* and *Pardofelis*

566 *temminckii* is consistent with an arboreal lifestyle. This is likely to reflect the

567 strong phylogenetic component observed in all humeral epiphyses, as these

568 species appear to be classified within the same group as their sister species

569 *Pardofelis marmorata* (Johnson et al., 2006). The same applies for *Felis*

570 *nigripes*, a species that one would expect to be classified as a terrestrial

571 species (cf. Meachen-Samuels & Van Valkenburgh, 2009), but is in fact

572 classified as a either 'Terrestrial but Climbs' or 'Terrestrial and Arboreal'. It is

573 likely that this species retained ancestral adaptations for climbing in humeral

574 morphology that are not needed for its current habitat preference (short

575 grassland of Southern Africa, (MacDonald et al., 2010).

576   In summary, we have found that whilst the shape of humeral epiphyses

577 is strongly informative of Felidae evolutionary history, size and locomotion exert

578 an adaptive influence on their interspecific shape variation. Our study provides

579 a solid baseline to extend two dimensional geometric morphometric analyses to

580 other long bone epiphyses, as well as other mammals.

581

582 **ACKNOWLEDGEMENTS**

596

597 **LITERATURE CITED**

598 Adams DC, Rohlf FJ, Slice DE. 2004. Geometric morphometrics: ten years of

599 progress following the 'revolution'. Ital J Zool 71:5–16.

600 Adams DC. 2008. Phylogenetic meta-analysis. Evolution 62:567–572.

601 Andersson KI, Werdelin L. 2003. The evolution of cursorial carnivores in the

602 Tertiary: implications of elbow-joint morphology. Proc Roy Soc Lond B (Suppl)

603 270:S163–S165.

604 Andersson KI. 2004. Elbow-joint morphology as a guide to forearm and foraging

605 behaviour in mammalian carnivores. Zool J Linn Soc 142:91–104.

606 Anyonge W. 1996. Locomotor behaviour in Plio-Pleistocene sabre-tooth cats: a

607 biomechanical analysis. J Zool 238:395–413.

608 Astúa D. 2009. Evolution of scapula size and shape in didelphid marsupials

609 (Didelphimorphia: Didelphidae). Evolution 63:2438–2456.

610 Bertram JEA, Biewener AA. 1990. Differential scaling of the long bones in the

611 terrestrial Carnivora and other mammals. J Morphol 204:157–169.

612 Bishop LC. 1999. Suid paleoecology and habitat preference at African Pliocene

613 and Pleistocene hominid localities. In: Bromage TG & Schrenk F, editors.

614 African Biogeography, Climate Change and Early Hominid Evolution. New York:

615 Oxford University Press. p 216–225.

616 Bookstein FL. 1989. Size and shape: a comment on semantics. Syst Zool

617 38:173–180.

618 Bookstein FL. 1991. Morphometric tools for landmark data. Geometry and

619 Biology. Cambridge: Cambridge University Press.

620 Cardini A, Elton S. 2007. Sample size and sampling error in geometric

621 morphometric studies of size and shape. Zoomorphology 126:121–134.

622   Carrano MT. 1999. What, if anything, is a cursor? Categories vs. continua for

623   determining locomotor habit in mammals and dinosaurs. J Zool 247:29–42.

624   Caumul R, Polly PD. 2005. Phylogenetic and environmental components of

625   morphological variation: skull, mandible, and molar shape in marmots

626   (Marmota, Rodentia). Evolution 57:2460–2472.

627   Chen X, Milne N, O' Higgins P. 2005. Morphological variation of the

628   thoracolumbar vertebrae in Macropodidae and its functional relevance. J

629   Morphol 266:167–181.

630   Christiansen P. 1999. Scaling of the limb long bones to bodymass in terrestrial

631   mammals. J Morphol 239:167–190.

632   Christiansen P. 2002. Mass allometry of the appendicular skeleton in terrestrial

633   mammals. J Morphol 251(2):195–209.

634   Christiansen P, Harris M. 2005. Body size of *Smilodon* (Mammalia: Felidae). J

635   Morphol 266:369–384.

636   Christiansen P. 2008. Evolution of skull and mandible shape in cats (Carnivora:

637   Felidae). PLoS ONE 3:e2807.

638   Clevedon Brown J, Yalden DW. 1973 The description of mammals-2 Limbs and

639   locomotion of terrestial mammals. Mammal Rev 3:107–134.

640   Day LM, Jayne BC. 2007. Interspecific scaling of the morphology and posture of

641   the limbs during the locomotion of cats (Felidae). J Exp Biol 210:642–654.

642   Diniz-Filho JAF, Nabout JC. 2009. Modeling body size evolution in Felidae

643   under alternative phylogenetic hypotheses. Genet Mol Biol 32:170–176.

644 Doube M, Wiktorowicz-Conroy A, Christiansen P, Hutchinson JR, Shefelbine S.

645 2009. Three-dimensional geometric analysis of felid limb bone allometry. PLoS

646 ONE 4:e4742.

647 Elton S. 2001. Locomotor and habitat classification of cercopithecoid postcranial

648 material from Sterkfontein Member4, Bolt's Farm and Swartkrans Members 1

649 and 2, South Africa. Palaeontologia africana 37:115–126.

650 Elton S. 2002. A reappraisal of the locomotion and habitat preference of

651 Theropithecus oswaldi. Folia Primatol 73:252–280.

652 Elton S. 2006. 40 years on and still going strong: the use of the hominin-

653 cercopithecid comparison in human evolution. J Roy Anthropol Inst 12:19–38.

654 Ewer RF. 1973. The carnivores. New York: Cornell University Press.

655 Gebo DL, Rose KD. 1993. Skeletal morphology and locomotor adaptation in

656 *Prolimnocyon atavus*. J Vertebr Paleont 13:125–144.

657 Gonyea WJ. 1976. Behavioural implications of saber-toothed felid morphology.

658 Paleobiology 2:332–342.

659 Holliday JA, Steppan SJ. 2004. Evolution of hypercarnivory: the effect of

660 specialization on morphological and taxonomic diversity. Paleobiology 30:108–

661 128.

662 Hughes JK, Elton S, & O'Regan HJ. 2008. Theropithecus and 'Out of Africa'

663 dispersals in the Plio-Pleistocene. J Hum Evol 54:43–77.

664 Johnson WE, Eizirik E, Pecon-Slattery J, Murphy WJ, Antunes A, Teeling E,

665 O'Brien SJ. 2006. The late Miocene radiation of modern Felidae: a genetic

666 assessment. Science 311:73–77.

667 Kappelman J. 1988. Morphology and locomotor adaptations of the bovid femur

668 in relation to habitat. J Morphol 198:19–130.

669 Kardong KV, Zalisko EJ. 2002. Comparative Vertebrate Anatomy: A Laboratory

670 Dissection Guide. Boston: McGraw-Hill.

671 Kitchener A. 1991. The Natural History of the Wild Cats. New York: Comstock

672 Publishing Associates.

673 Kitchener AC, Van Valkenburgh B, Yamaguchi N. 2010. Felid form and function.

674 In: MacDonald DW, Loveridge AJ, editors. Biology and Conservation of Wild

675 Felids. Oxford: Oxford University Press. p 83–106.

676 Kovarovic K, Aiello LC, Cardini A, Lockwood CA. 2011. Discriminant Function

677 Analysis in archaeology: are classification rates too good to be true? J Archaeol

678 Sci 38:3006–3018.

679 Lencastre Sicuro F. 2011. Evolutionary trends on extant cat skull morphology

680 (Carnivora: Felidae): a three-dimensional geometrical approach. Biol J Linn Soc

681 103:176–190.

682 Lencastre Sicuro F, Oliveira FB. 2011. Skull morphology and functionality of

683 extant Felidae (Mammalia: Carnivora): a phylogenetic and evolutionary

684 perspective. Zool J Linn Soc 161:414–462.

685 Lewis ME, Lague MR. 2010. Interpreting sabretooth cat (Carnivora; Felidae;

686 Machairodontinae) postcranial morphology in light of scaling patterns. In:

687 Goswami A, Friscia AR, editors. Carnivoran Evolution. New views on

688 phylogeny, form and function. Cambridge: Cambridge University Press. p 411–

689 465.

690 MacDonald DW, Loveridge AJ, Nowell K. 2010. *Dramatis personae*: an

691 introduction to the wild felids. In: MacDonald DW, Loveridge AJ, editors. Biology

692 and Conservation of Wild Felids. Oxford: Oxford University Press Oxford. p 3–

693 58.

694 Maddison DR, Maddison WP. 2000. MacClade version 4: Analysis of phylogeny

695 and character evolution. Sinauer Associates, Sunderland Massachusetts.

696 Martins EP, Hansen TF. 1997. Phylogenies and the comparative method: a

697 general approach to incorporating phylogenetic information into the analysis of

698 interspecific data. Am Nat 149:646–667.

699 Mattern MY, McLennan DA. 2000. Phylogeny and speciation of felids. Cladistics

700 16:232–253.

701 Meachen-Samuels J, Van Valkenburgh B. 2009a. Forelimb indicators of prey-

702 size preference in the Felidae. J Morphol 270:729–744.

703 Meachen-Samuels J, Van Valkenburgh B. 2009b. Craniodental indicators of

704 prey size preference in the Felidae. Biol J Linn Soc 96:784–799.

705 Meachen-Samuels J, Van Valkenburgh B. 2010. Radiographs reveal

706 exceptional forelimb strength in the sabertooth cat, Smilodon fatalis. PLoS ONE

707 5:e11412.

708 Meachen-Samuels J. 2012. Morphological convergence of the prey-killing

709 arsenal of sabertooth predators. Paleobiology 38:1–14.

710 Meloro C, Raia P, Piras P, Barbera C, O'Higgins P. 2008. The shape of the

711 mandibular corpus in large fissiped carnivores: allometry, function and

712 phylogeny. Zool J Linn Soc 154:832–845.

713   Meloro C. 2011a. Feeding habits of Plio-Pleistocene large carnivores as

714   revealed by their mandibular geometry. J Vertebr Paleont 31:428–446.

715   Meloro C. 2011b. Morphological disparity in Plio-Pleistocene large carnivore

716   guilds from Italian peninsula. Acta Palaeontol Pol 56:33–44.

717   Meloro C. 2011c. Locomotor adaptations in Plio-Pleistocene large carnivores

718   from the Italian peninsula: Palaeoecological implications. Current Zoology

719   57:269–283.

720   Meloro C, O' Higgins P. 2011. Ecological adaptations of mandibular form in

721   fissiped Carnivora. J Mamm Evol 18:185–200.

722   Meloro C, Raia P, Carotenuto F, Cobb S. 2011. Phylogenetic signal, function

723   and integration in the subunits of the carnivoran mandible. Evol Biol 38:465–

724   475.

725   Monteiro LR. 1999. Multivariate regression models and geometric

726   morphometrics: the search for causal factors in the analysis of shape. Syst Biol

727   48:192–199.

728   Monteiro LR, Abe AS. 1999. Functional and historical determinants of shape in

729   the scapula of Xenarthran mammals: evolution of a complex morphological

730   structure. J Morphol 241:251–263.

731   O' Higgins P, Jones N. 2006. Morphologika 2.5, York: Function morphology &

732   evolution research group, Hull York Medical School.

733   Ortolani A, Caro TM. 1996. The adaptive significance of color patterns in

734   carnivores: phylogenetic tests of classic hypotheses. In: Gittleman JL, editor.

735   Carnivore Behaviour, Ecology, and Evolution, Vol. 2. New York: Cornell

736   University Press. p 132–188.

737   Plummer TW, Bishop LC. 1994. Hominid Paleoecology at Olduvai Gorge,

738   Tanzania as indicated by antelope remains. J Hum Evol 27:47–75.

739   Polly PD, Macleod N. 2008. Locomotion in fossil carnivora: an application of

740   eigensurface analysis for morphometric comparison of 3D surfaces.

741   Palaeontologia Electronica 11.2.8A.

742   Radinsky LB. 1981. Evolution of skull shape in carnivores, 1: representative of

743   modern carnivores. Biol J Linn Soc 15:369–388.

744   Reighard JE, Jennings, HS. 1901. Anatomy of the Cat. New York: H. Holt.

745   Rohlf FJ. 1996. Morphometric spaces, shape components and the effect of

746   linear transformations. In: Marcus LF, Corti M, Loy A, et al., editors. Advances

747   in morphometrics. New York: Plenum Press. p 131–129.

748   Rohlf FJ. 2000. On the use of shape spaces to compare morphometric

749   methods. Hystrix Ital J Mamm 11:8–24.

750   Rohlf FJ. 2001. Comparative methods for the analysis of continuous variables:

751   geometric interpretations. Evolution 55:2143–2160.

752   Rohlf FJ. 2003a. Bias and error in estimates of mean shape in morphometrics. J

753   Hum Evol 44:665–683.

754   Rohlf FJ. 2003b. tpsSmall1.20. Stony Brook, NY: Department of Ecology and

755   Evolution, State University of New York.

756   Rohlf FJ. 2006a. A comment on phylogenetic correction. Evolution 60:1509–

757   1515.

758   Rohlf FJ. 2006b. NTSYSpc 2.21c. New York: Exeter Software.

759   Rohlf FJ. 2008. tpsDig2.12. Stony Brook, NY: Department of Ecology and

760   Evolution, State University of New York.

761 Rohlf FJ. 2009. tpsRegr1.37. Stony Brook, NY: Department of Ecology and

762 Evolution, State University of New York.

763 Slater GJ, Van Valkenburgh B. 2008. Long in the tooth: evolution of sabertooth

764 cat cranial shape. Paleobiology 34:403–419.

765 Samuels JX, Van Valkenburgh B. 2008. Skeletal indicators of locomotor

766 adaptations in living and extinct rodents. J Morphol 269:1387–1411.

767 Schutz H, Guralnick RP. 2007. Postcranial element shape and function:

768 assessing locomotor mode in extant and extinct mustelids carnivorans. Zool J

769 Linn Soc 150: 895–914.

770 SPSS Inc. 2009. PASW Statistics 18.0. Chicago: IBM company headquarters.

771 Turner A, Antón M. 1997. The Big Cats and their fossil relatives. New York:

772 Columbia University Press.

773 Van Valkenburgh B. 1987. Skeletal Indicators of Locomotor Behaviour in Living

774 and Extinct Carnivores. J Vertebr Paleont 7:162–182.

775 Werdelin L. 1983. Morphological patterns in the skulls of cats. Biol J Linn Soc

776 19:375–391.

777 Werdelin L, Wesley-Hunt G. 2010. The biogeography of carnivore

778 ecomorphology. In: Goswami A, Friscia A, editors. Carnivoran Evolution: New

779 Views on Phylogeny, Form and Function. New York: Cambridge University

780 Press. p 225–245.

781 Werdelin L, Yamaguchi N, Johnson WE, O'Brien SJ. 2010. Phylogeny and

782 evolution of cats (Felidae). In: MacDonald DW, Loveridge AJ, editors. Biology

783 and Conservation of Wild Felids. Oxford: Oxford University Press. p 59–82.

784 Young, N.M. 2008. A Comparison of the Ontogeny of Shape Variation in the

785 Anthropoid Scapula: Functional and Phylogenetic Signal. American Journal of

786 Physical Anthropology. 136:247–264.

787 Zelditch ML, Swiderski DL, Sheets HD, Fink WL. 2004. Geometric

788 morphometrics for biologists. A primer. Amsterdam: Elsevier.

789

790

791 **FIGURE CAPTIONS**

792 **Fig. 1** The location of landmarks digitised for each epiphyseal aspect.

793 Landmarks are placed to represent anatomical loci of functional significance.

794 Scale bars represent 10 millimetres. Dotted lines demonstrate how angular and

795 linear measurements were used to obtain landmarks geometrically. A = Lateral

796 aspect of the proximal epiphysis, B = Medial aspect of the proximal epiphysis, C

797 = Anterior aspect of the distal epiphysis, D = Posterior aspect of the distal

798 epiphysis. Anatomical position of each landmark as follows: (A1, B1) Most distal

799 point on the humeral head; (A2) proximal junction between humeral head and

800 greater tubercle; (A3*) lies on the anterior surface of the humerus and is

801 perpendicular to the line connecting landmarks A1 & A2, at the level of

802 landmark A2; (A4, B8) proximal tip of the greater tubercle; (A5*) furthest

803 projection of the humeral head, at a distance halfway between landmarks A1 &

804 A2; (B2) most anterior and most distal point on the lesser tubercle; (B3) most

805 anterior and most proximal point on the lesser tubercle; (B4*) lies on the

806 anterior surface of the humerus and is perpendicular to the line connecting

807 landmarks B1 & B3, at the level of landmark B3; (B5) most posterior and most

808 distal point on the lesser tubercle; (B6) most posterior and most proximal point

809 on the lesser tubercle; (B7*) furthest projection of the humeral head at a

810 distance halfway between landmarks B1 & B6; (C1, D2) distal tip of the

811 trochlea; (C2, D3) distal junction between the trochlea and capitulum; (C3, D4)

812 most distal and most lateral point on the capitulum; (C4, D1) most proximal and

813 most lateral point on the capitulum; (C5) proximal tip of the trochlea; (C6)

814 proximal tip of the supracondyloid foramen; (C7, D7) most medial point on the

815 medial epicondyle; (D5) proximal tip of the olecranon fossa; (D6) most lateral

816 point on the lateral epicondyle; (D8*) lies on the medial surface of the olecranon

817 fossa and is perpendicular to the line connecting landmark D1 & D4, at the level

818 of landmark D1. *Landmark obtained geometrically.

819

820 **Fig. 2** Four PC plots describing the scatter of specimens across PC1 and PC2.

821 Each PC plot represents a different epiphyseal aspect; A= Lateral aspect of the

822 proximal epiphysis, B= Medial aspect of the proximal epiphysis, C= Anterior

823 aspect of the distal epiphysis, D= Posterior aspect of the distal epiphysis.

824 Specimens are grouped according to lineage. Transformation grids, at the

825 extremes of each PC, show the relative deformation from the mean shape.

826 Landmarks are linked by a wireframe in all transformation grids.

827

828 **Fig. 3** Transformation grids to demonstrate the relative change in shape from

829 the smallest to the median and to the largest value of NLog centroid size for

830 each epiphyseal aspect. Centroid sizes given in each grid are to 3 significant

831 figures. Letters indicate epiphyseal aspect: A= Lateral aspect of the proximal

832 epiphysis, B= Medial aspect of the proximal epiphysis, C= Anterior aspect of the

833 distal epiphysis, D= Posterior aspect of the distal epiphysis. The smallest NLog

834 centroid size is exhibited by an individual of the species *Prionailurus planiceps*

835 in all cases, excluding the anterior aspect of the distal epiphysis, where the

836 smallest value is provided by a specimen of the species *Felis nigripes*.

837 Specimens of *Caracal caracal* represent the median NLog centroid size in the

838 case of the lateral and medial views of the proximal epiphysis. In the case of the

839 distal epiphysis, specimens are of *Lynx lynx*. Finally, the largest NLog centroid

840 size values are provided by specimens belonging to the species *Panthera leo* in

841 the case of the proximal epiphysis. These values are provided by *Panthera*

842 *tigris* specimens for the distal epiphysis.

843

844 **Fig. 4** Four plots of function 1 vs. function 2 determined by DFAs. The scatter of

845 specimens, categorised according to locomotor group, is shown, with group

846 centroids included. Each plot represents a different epiphyseal aspect; A=

847 Lateral aspect of the proximal epiphysis, B= Medial aspect of the proximal

848 epiphysis, C= Anterior aspect of the distal epiphysis, D= Posterior aspect of the

849 distal epiphysis. Transformation grids, at the extremes of each axis, show the

850 relative deformation from the mean shape. Landmarks are linked by a

851 wireframe in all transformation grids.

852

853 **Fig. 5.** Composite phylogeny of 32 extant species of Felidae showing character

854 mapping based on squared-change parsimony (Maddison and Maddison, 2000)

855   for PC1 species-averaged scores of the four epiphyses analysed. Time of

856   divergence between species are expressed in millions of years.

857   A= Lateral aspect of the proximal epiphysis, B= Medial aspect of the proximal

858   epiphysis, C= Anterior aspect of the distal epiphysis, D= Posterior aspect of the

859   distal epiphysis.

A

0.322   1.287   2.224

B

0.391   1.374   2.312

C

0.439   1.342   2.290

D

0.321   1.274   2.250

● Terrestrial
● Terrestrial and Arboreal
○ Terrestrial but Climbs
⅄ Ungrouped
✳ Group Centroid
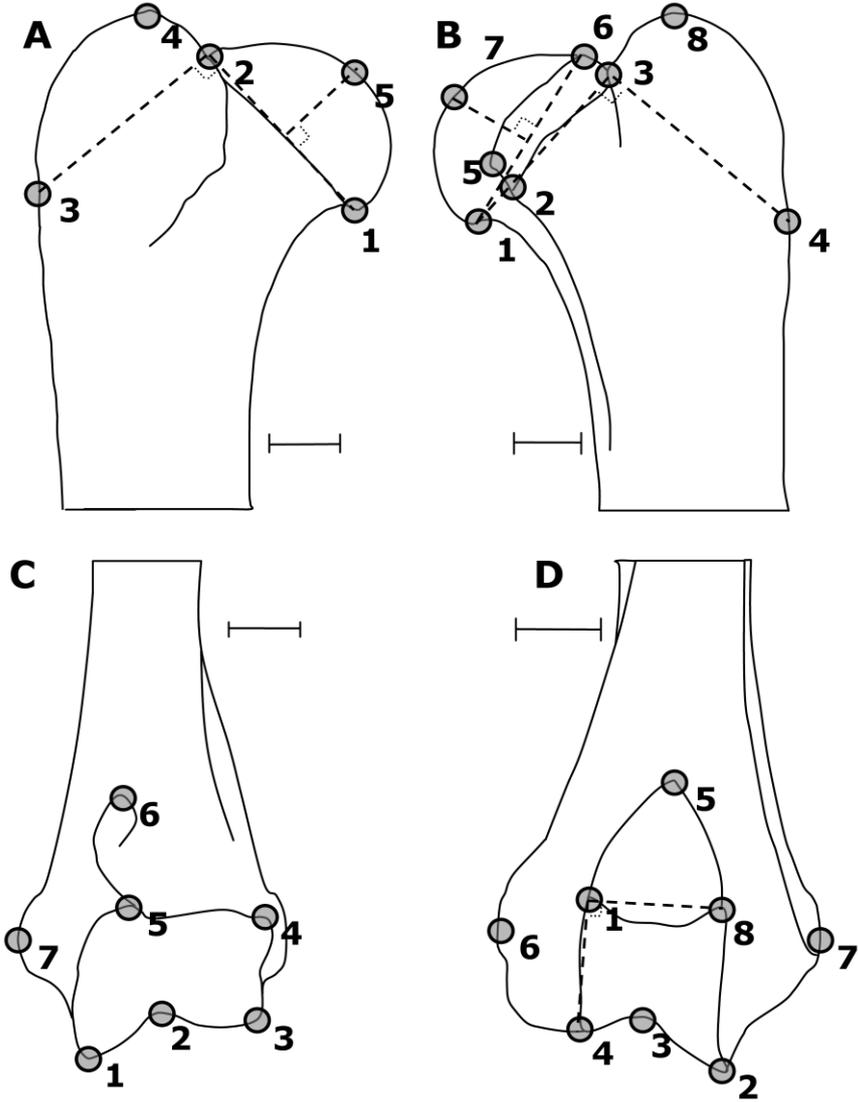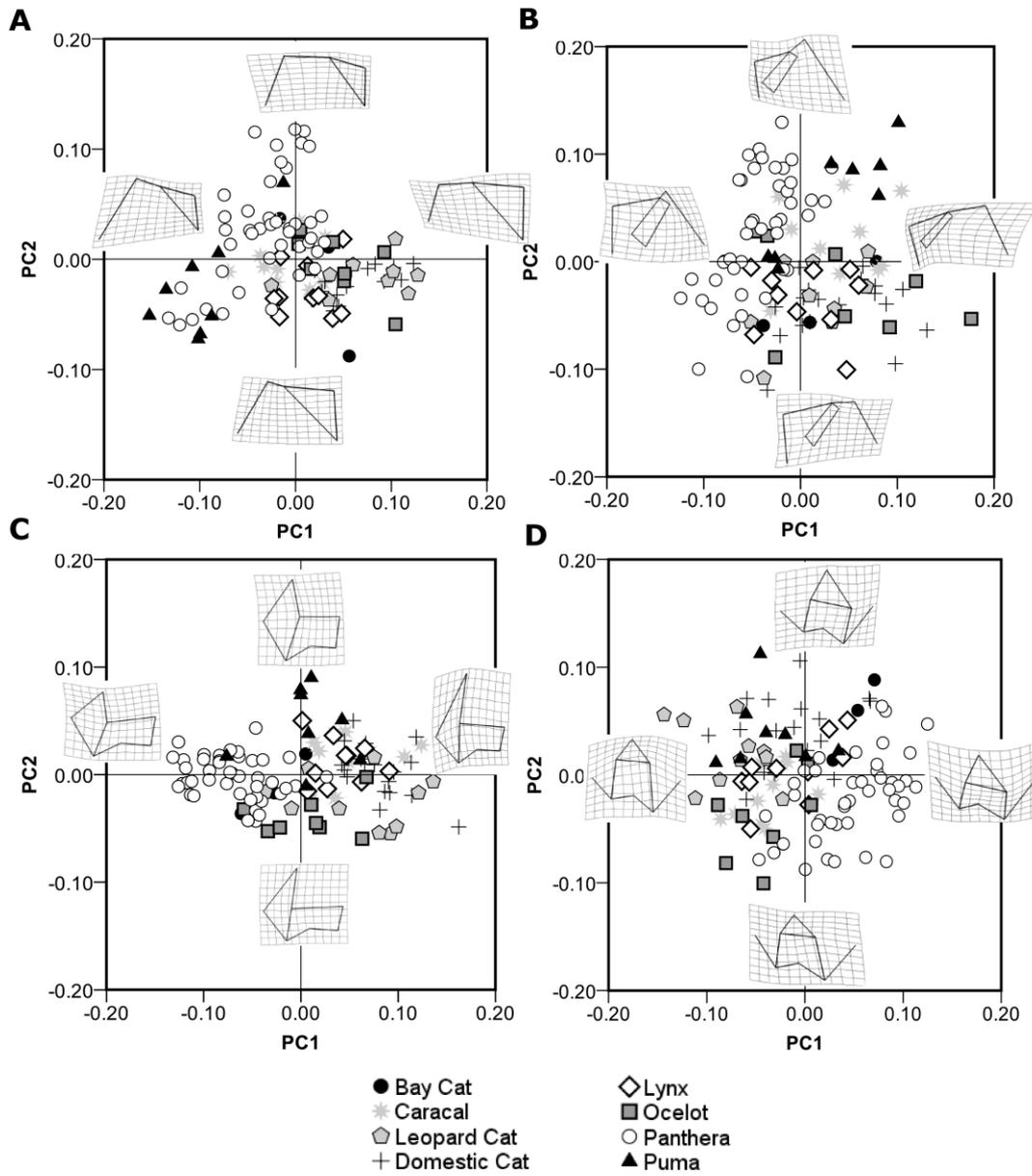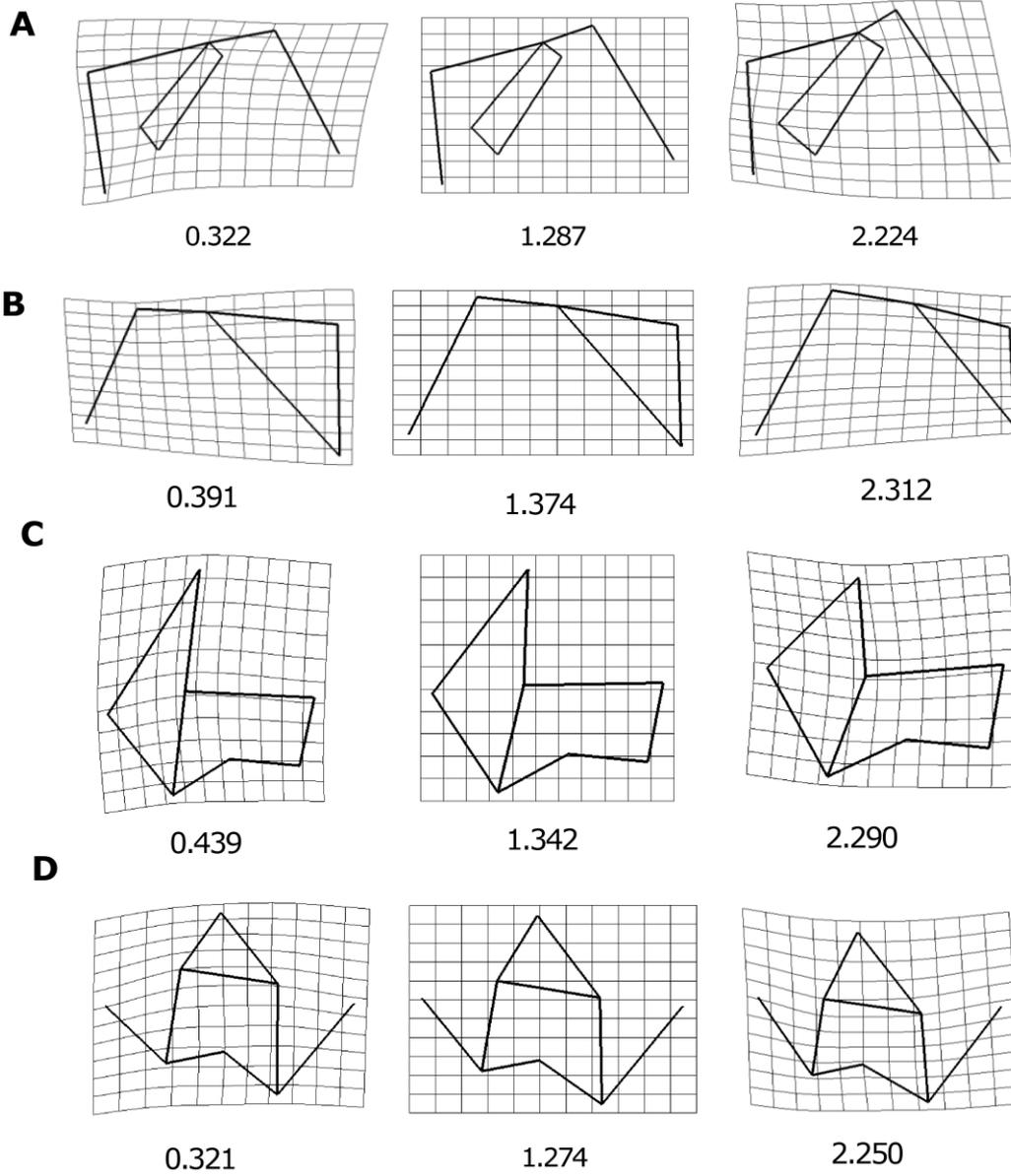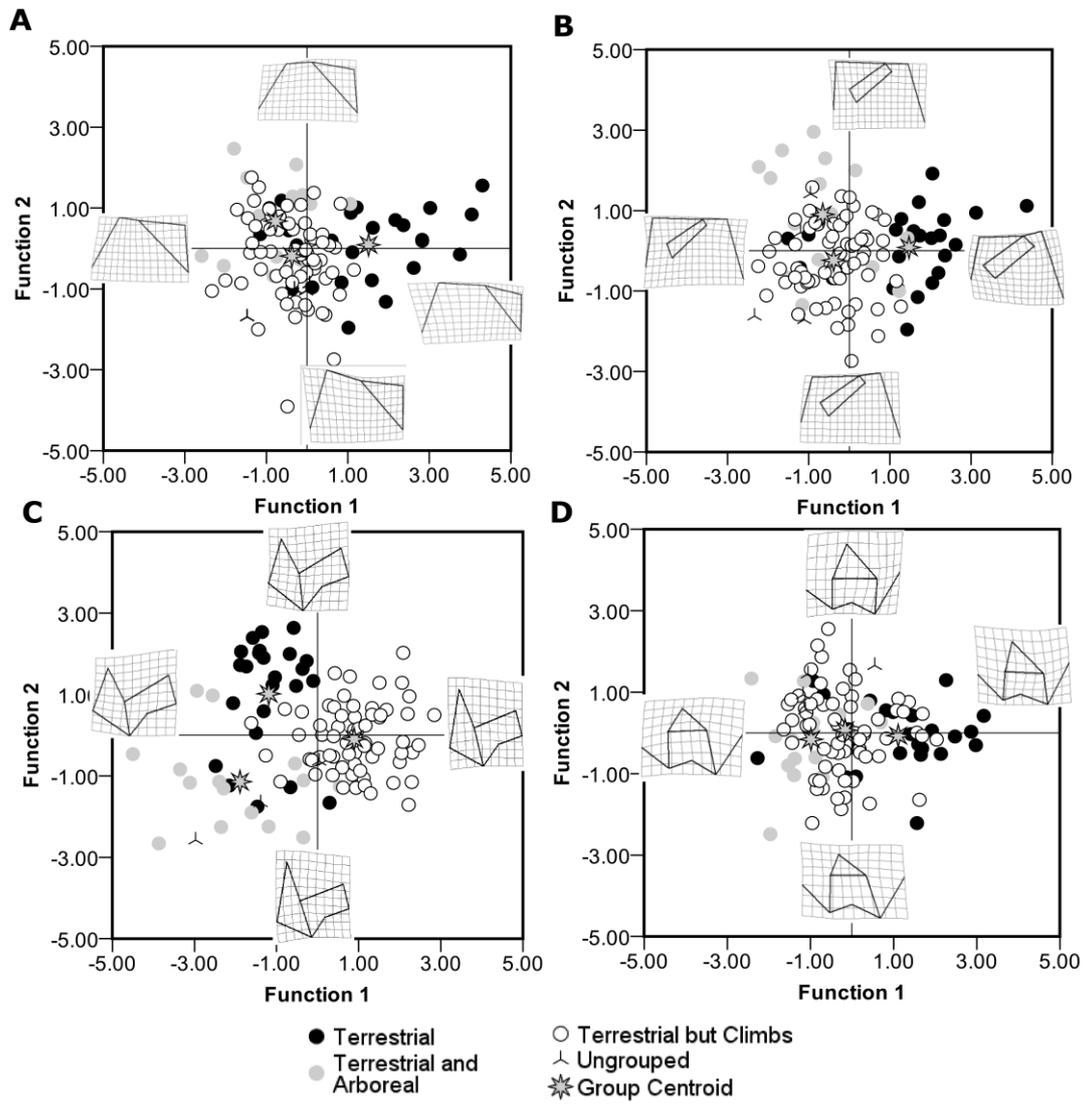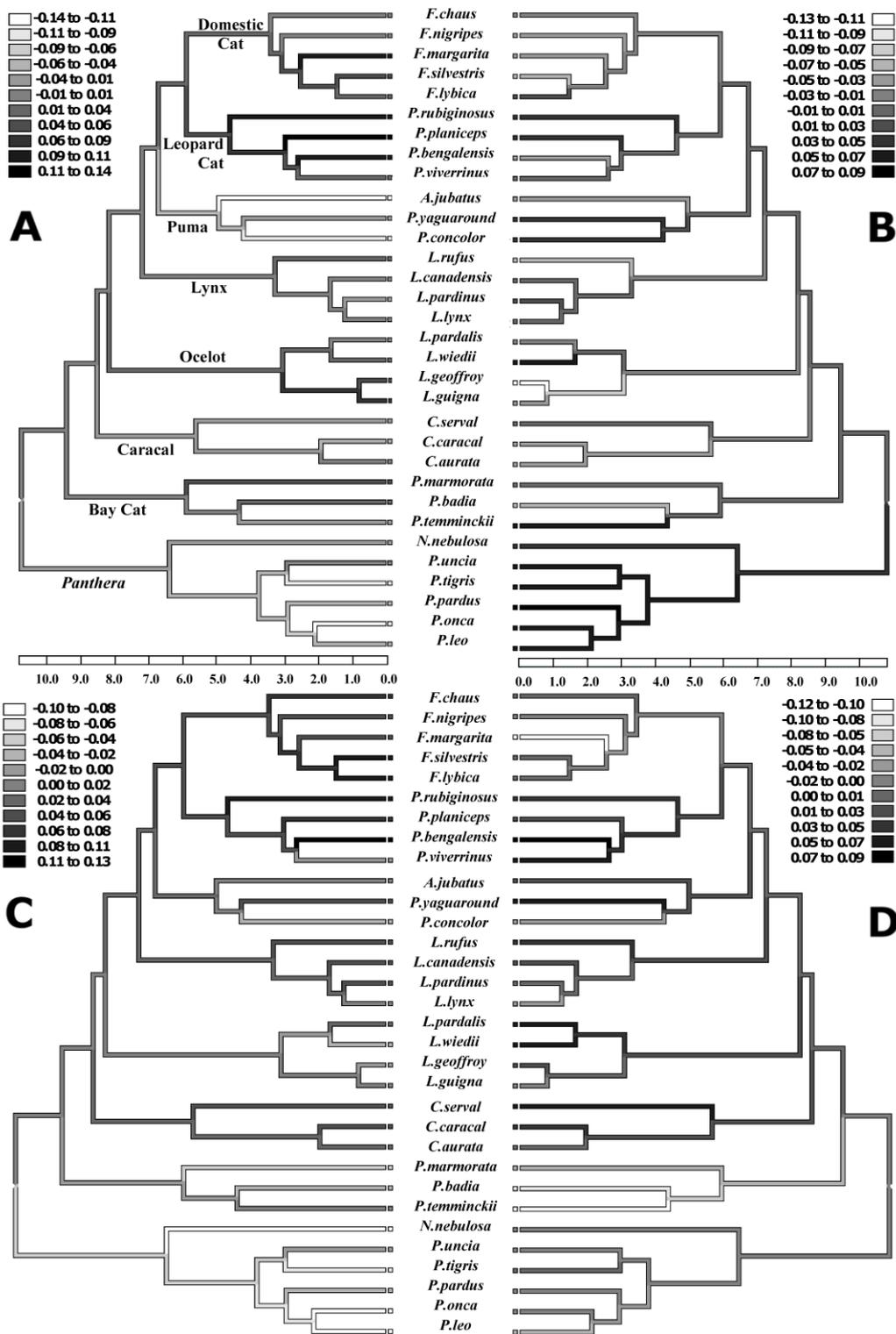
TABLES

Table 1 MANOVA statistic for each epiphyseal aspect, with phylogenetic categories as independent (X) and shape PCs as the dependent (Y) variables. The percentage of variance explained by phylogeny is displayed for each aspect. Significant P values are highlighted in bold.

Epiphysis and aspect	Wilks' Lambda	F	Hypo d.f.	Error d.f.	% variance explained	P value
Lateral aspect, proximal epiphysis	0.140	5.632	42	453.7	45.67	**<0.0001**
Medial aspect, proximal epiphysis	0.032	5.050	84	559.2	33.97	**<0.0001**
Anterior aspect, distal epiphysis	0.045	5.517	70	549.1	53.20	**<0.0001**
Posterior aspect, distal epiphysis	0.028	5.326	84	565.3	35.67	**<0.0001**

Table 2 Statistic for multivariate regression testing allometry with Nlog size as independent (X) variable and shape PCs as dependent (Y). The percentage of variance explained by size is displayed for each epiphyseal aspect. Significant

Epiphysis and aspect	Wilks' Lambda	F	Hypo d.f.	Error d.f.	% variance explained	P value
Lateral aspect, proximal epiphysis	0.272	45.533	6	102	35.35	**<0.0001**
Medial aspect, proximal epiphysis	0.207	30.568	12	96	20.07	**<0.0001**
Anterior aspect, distal epiphysis	0.260	28.150	10	99	40.17	**<0.0001**
Posterior aspect, distal epiphysis	0.205	31.394	12	97	17.01	**<0.0001**

P values are highlighted in bold.

Table 3 MANOVA statistic for each epiphyseal aspect with locomotion categories as independent (X) variables and all shape PCs as the dependent (Y). The percentage of variance explained by locomotion is displayed for each aspect. Significant P values are highlighted in bold. *Pardofelis temminckii*, *Pardofelis badia* and 2 of *Felis nigripes*, were excluded from MANOVA as the locomotor category of these individuals is unknown

Epiphysis and aspect	Wilks' Lambda	F	Hypo d.f.	Error d.f.	% variance explained	P value
Lateral aspect, proximal epiphysis	0.490	6.927	12	194	11.70	**<0.0001**
Medial aspect, proximal epiphysis	0.449	3.731	24	182	4.83	**<0.0001**
Anterior aspect, distal epiphysis	0.360	6.268	20	188	16.09	**<0.0001**
Posterior aspect, distal epiphysis	0.494	3.239	24	184	8.96	**<0.0001**

Table 4 Wilks' Lambda values in addition to degrees of freedom and P values for both functions created in each DFA. Significant P values are highlighted in bold.

Epiphysis and aspect	Function	Wilks' Lambda	d.f.	P value
Lateral aspect, proximal epiphysis	DF1	0.535	6	**<0.0001**
	DF2	0.916	2	**0.012**
Medial aspect, proximal epiphysis	DF1	0.518	10	**<0.0001**
	DF2	0.864	4	**0.006**
Anterior aspect, distal epiphysis	DF1	0.288	12	**<0.0001**
	DF2	0.690	5	**<0.0001**
Posterior aspect, distal epiphysis	DF1	0.682	6	**<0.0001**
	DF2	0.992	2	0.681

Table 5 The composition of each function, showing the variables selected by stepwise procedure and the correlation coefficient (r) loaded on each function. NLog_CS = NLog centroid size, PC = Principal Component of shape variables.

Epiphysis and aspect	Function 1	Function 2
Lateral aspect, proximal epiphysis	PC2 0.793	PC3 0.819 PC6 0.561
Medial aspect, proximal epiphysis	PC7 0.589 NLog_CS 0.571 PC4 0.284	PC8 0.798 PC9 0.307
Anterior aspect, distal epiphysis	PC9 0.340	NLog_CS 0.731 PC1 -0.444 PC4 -0.439 PC8 0.321 PC3 0.285
Posterior aspect, distal epiphysis	NLog_CS 0.725	PC2 0.756 PC7 -0.650

Table 6 Percentage of correctly classified cases after leave one out procedure, including an overall percentage for each epiphyseal aspect, and specific percentages for each locomotor group.

Epiphysis and aspect	Total %	%Terrestrial	% Terrestrial and Arboreal	% Terrestrial but Climbs
Lateral aspect, proximal epiphysis	62.9	75.0	60.0	59.1
Medial aspect, proximal epiphysis	64.8	83.3	60.0	59.1
Anterior aspect, distal epiphysis	83.0	79.2	62.5	89.4
Posterior aspect, distal epiphysis	50.0	66.7	62.5	40.9

Table 7 Percentage of correctly reclassified specimens for each species in LAPE (lateral aspect of the proximal epiphysis), MAPE (medial aspect of the proximal epiphysis), AADE (anterior aspect of the distal epiphysis) and PADE (posterior aspect of the distal epiphysis). Predicted locomotor categories for the unknown specimens by each DFA are also listed in the table (T but Cl = Terrestrial but Climbs; T and A = Terrestrial and Arboreal). # prox = Number of proximal specimens per species. # dist = Number of distal specimens per species

Species	# prox	# dist	LAPE	MAPE	AADE	PADE
Acinonyx jubatus	5	5	**100.00%**	**100.00%**	80.00%	40.00%
Caracal aurata	2	2	**100.00%**	0.00%	**100.00%**	50.00%
Caracal caracal	2	2	50.00%	50.00%	**100.00%**	**100.00%**
Caracal serval	6	6	50.00%	83.33%	**100.00%**	0.00%
Felis silvestris lybica	3	3	**100.00%**	33.33%	**100.00%**	33.33%
Felis chaus	2	2	**100.00%**	50.00%	**100.00%**	50.00%
Felis margarita	2	2	0.00%	0.00%	0.00%	0.00%
Felis nigripes	2	2	T but Cl	T but Cl	T but Cl	T but Cl
Felis silvestris grampia	9	9	44.44%	66.67%	**100.00%**	22.22%
Leopardus geoffroy	2	2	**100.00%**	50.00%	**100.00%**	50.00%
Leopardus guigna	1	1	0.00%	**100.00%**	**100.00%**	**100.00%**
Leopardus pardalis	4	4	75.00%	25.00%	75.00%	25.00%

Leopardus wiedii	1	1	0.00%	**100.00%**	**100.00%**	**100.00%**
Lynx lynx	3	3	33.33%	**100.00%**	**100.00%**	66.67%
Lynx rufus	1	1	**100.00%**	**100.00%**	**100.00%**	0.00%
Lynx canadensis	4	4	0.00%	0.00%	**100.00%**	50.00%
Lynx pardinus	2	2	**100.00%**	50.00%	50.00%	50.00%
Neofelis nebulosa	3	3	33.33%	33.33%	**100.00%**	**100.00%**
Panthera leo	17	17	**100.00%**	**100.00%**	**100.00%**	94.12%
Panthera onca	3	3	**100.00%**	0.00%	0.00%	0.00%
Panthera pardus	12	12	66.67%	50.00%	83.33%	58.33%
Panthera tigris	4	4	0.00%	50.00%	**100.00%**	25.00%
Panthera uncia	4	4	**100.00%**	**100.00%**	75.00%	50.00%
Pardofelis badia	1	1	T but Cl	T and A	T and A	T and A
Pardofelis marmorata	1	1	**100.00%**	**100.00%**	**100.00%**	**100.00%**
Pardofelis temminckii	1	1	T but Cl	T and A	T but Cl	T and A
Prionailurus bengalensis	3	4	33.33%	**100.00%**	33.33%	66.67%
Prionailurus planiceps	1	1	0.00%	0.00%	0.00%	0.00%
Prionailurus rubiginosus	1	1	**100.00%**	**100.00%**	**100.00%**	**100.00%**
Prionailurus viverrinus	4	4	25.00%	75.00%	50.00%	0.00%
Puma concolor	2	2	0.00%	50.00%	50.00%	**100.00%**
Puma jagouaroundi	1	1	0.00%	**100.00%**	**100.00%**	0.00%

Table 8 Percentage of correctly classified cases after leave one out procedure with specimens of *Panthera leo, Felis silvestris* or *Neofelis nebulosa* individually excluded, including an overall percentage for each epiphyseal aspect, and specific percentages for each locomotor group. # Sample prox/dist = Number of specimens used in proximal epiphyseal analyses / Number of specimens used in distal epiphyseal analyses

	Epiphysis and aspect	Total %	%Terrestrial	% Terrestrial and Arboreal	% Terrestrial but Climbs
Excluding *P.leo.* # Sample prox/dist = 88/89	Lateral aspect, proximal epiphysis	54.5	71.4	53.3	53.0
	Medial aspect, proximal epiphysis	56.8	71.4	46.7	57.6
	Anterior aspect, distal epiphysis	83.1	85.7	56.3	89.4
	Posterior aspect, distal epiphysis	59.6	57.1	31.3	66.7
Excluding *F.silvestris* # Sample prox/dist = 96/97	Lateral aspect, proximal epiphysis	69.8	75.0	60.0	70.2
	Medial aspect, proximal epiphysis	62.5	70.8	60.0	59.6
	Anterior aspect, distal epiphysis	81.4	79.2	62.5	87.7
	Posterior aspect, distal epiphysis	58.8	66.7	56.3	56.1
Excluding *N.nebulosa* # Sample prox/dist = 102/103	Lateral aspect, proximal epiphysis	67.6	75.0	58.3	66.7
	Medial aspect, proximal epiphysis	69.6	75.0	66.7	68.2
	Anterior aspect, distal epiphysis	81.6	79.2	61.5	86.4
	Posterior aspect, distal epiphysis	64.1	66.7	61.5	63.6

Table 9 Phylogenetic Generalised Least Squares models for locomotor categories or allometry, showing Wilks' Lambda, F test, degrees of freedom and probability values. Significant P values are highlighted in bold.

	Epiphysis and aspect	Wilks' Lambda	F	d.f. 1	d.f. 2	P value
PGLS Locomotion	Lateral aspect, proximal epiphysis	0.385	2.448	12.0	48.0	**0.0141**
	Medial aspect, proximal epiphysis	0.371	0.961	24.0	36.0	0.5317
	Anterior aspect, distal epiphysis	0.228	2.186	20.0	40.0	**0.0174**
	Posterior aspect, distal epiphysis	0.199	1.864	24.0	36.0	**0.0442**
PGLS Size	Lateral aspect, proximal epiphysis	0.403	6.169	6.0	25.0	**0.0005**
	Medial aspect, proximal epiphysis	0.234	5.179	12.0	19.0	**0.0008**
	Anterior aspect, distal epiphysis	0.494	2.147	10.0	21.0	0.0674
	Posterior aspect, distal epiphysis	0.191	6.708	12.0	19.0	**0.0001**